DOI: 10.1002/ejoc.200500544

BisPNA Targeting to DNA: Effect of Neutral Loop on DNA Duplex Strand Invasion by *aep*PNA-N7G/*aep*PNA-C Substituted Peptide Nucleic Acids

Pravin S. Shirude,[a] Vaijayanti A. Kumar,*[a] and Krishna N. Ganesh*[a]

Dedicated to Professor W. J. Stec on the occasion of his 65th birthday

Keywords: Peptide Nucleic Acid (PNA) / Hairpin bisPNA-DNA triplex / Strand invasion / *aep*PNA / N7G PNA

N7-Alkyl-substituted guanine (N7G) as a CH^+ mimic has been introduced into aminoethylglycyl PNA (*aeg*PNA) forming a hairpin through a neutral linker derived from bis(tetraethylene) glycol (*teg-teg*). These form pH-independent PNA_2:DNA triplexes with complementary DNA sequences. The introduction of chiral, cationic aminoethylprolyl (*aep*) units with C and the CH^+ mimic N7G in the backbone of the hairpin bisPNAs with a neutral *teg-teg* linker, influenced the recognition of complementary DNA in an orientation-selective manner. Fluorescence assay was used to examine the process of strand invasion of the target DNA duplex by the modified hairpin bisPNAs with the neutral *teg* linker and comparison of results of previous studies employing cationic linkers suggested the triplex formation to be a two-step process, with the preferred formation of HG bonds in the first step.

The acyclic, neutral and achiral aminoethylglycyl (*aeg*) PNAs hybridize to complementary oligonucleotides with high affinity and specificity through Watson–Crick base pairing and are true mimics in terms of base-pair recognition.[1] The unique properties of peptide nucleic acids (PNAs)[2,3] as novel molecules designed to bind effectively with high sequence specificity to desired double-stranded DNA (dsDNA) targets through duplex invasion have attracted wide attention, warranting molecular characterization of binding mechanisms. PNA can bind to complementary nucleic acids with Watson–Crick (WC) pairing in both antiparallel (*ap*) and parallel (*p*) orientations,[4] but with slightly preferred antiparallel binding.[5] Homopyrimidine oligomers such as PNA-C_{10} or PNA-$(CT)_5$ invade double stranded polynucleotides by forming PNA_2:DNA triplexes in a pH-dependent reaction, owing to the necessity of protonation of N3 in cytosine in the third strand. Several attempts have been made in the literature to imitate the CH^+---C hydrogen-bonding pattern by neutral mimics[6–15] such as N7G (G glycosylated at N7), 8-oxo-adenine, pseudoisocytosine (ψiC)[7] and the J base to avoid the necessity of acidic pH for triplex formation by C-containing PNA oligomers. Such systems exhibit pH-independent triplex formation.

In PNA_2:DNA triplexes, where the DNA strand is engaged in simultaneous binding to two PNA strands, ambiguity persists in establishing the specific correlation among the parallel/antiparallel PNA strands with the Hoogsteen (HG) or Watson–Crick (WC) binding modes (Figure 1) with DNA.[16] In principle, PNA_2:DNA triplexes are possible with different combinations of parallel/antiparallel strands that are not easily discernible.

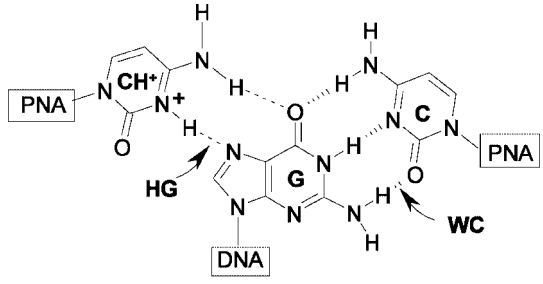

Figure 1. H-bonding in PNA_2:DNA triplex: HG (Hoogsteen), WC (Watson–Crick).

The ambiguity in PNA strand orientation for WC and HG binding with DNA in such mixed PNA_2:DNA complexes can be partially resolved by conjugating the two PNA strands with a linker to construct a bisPNA hairpin that can form only two triplexes with a 1:1 (PNA:DNA) composition[13] (Figure 2). To identify each of these possibilities, we introduced the chiral aminoethylprolyl (*aep*) [(2*S*,4*S*)-*aep*PNA C and N7G] units into arm A, which is linked to arm B of the bisPNA through a cationic peptide

[a] Division of Organic Chemistry (Synthesis), National Chemical Laboratory,
Pune 411008, India
E-mail: kn.ganesh@ncl.res.in, va.kumar@ncl.res.in

Supporting information for this article is available on the WWW under http://www.eurjoc.org or from the author.

linker.[8] This was hybridized to DNA sequences designed to specifically recognise arm A in either parallel or antiparallel mode. We found that bisPNAs consisting of chiral *aep*PNA-C or *aep*PNA-N7G in arm A, formed triplexes with higher stability when this arm was antiparallel to the DNA strand. As expected, the triplex formation was pH independent with *aep*PNA-N7G, while pH dependent with the bisPNA *aep*PNA-C. The presence of lysines in the peptide linker renders bisPNAs inherently cationic, which may disfavor N3-protonation in *aep*PNA-C that is necessary for HG bonding. The positive charges in the linker may also accelerate the PNA:DNA hybridization kinetics making analysis of the relative contributing factors to triplex stability unambiguous.

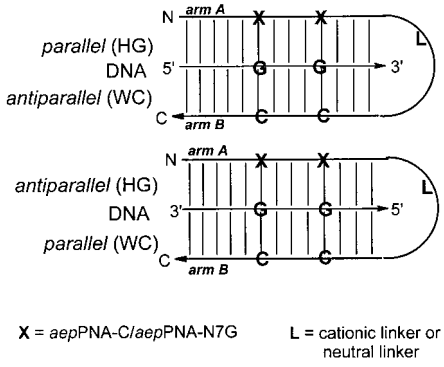

Figure 2. Triplex formation with bisPNAs carrying N7G as a neutral C^+ mimic.

In this report, we have replaced the charged peptide linker[8] with a neutral linker (Figure 2) composed of two tetraethylene glycol units to examine the true preferences in hybridization of the two arms of PNA containing *aep*PNA-C or *aep*PNA-N7G in parallel/antiparallel orientation to the DNA strand (Figure 3). The hairpin PNAs (H-TTTXTXT-*teg*-*teg*-TCTCTTT-β-alanine), containing the neutral bis(tetraethylene) glycol (*teg*) linker along with *aep*PNA-C or *aep*PNA-N7G in the X position, enable the study of hybridization preferences with complementary DNA by UV-T_m at different pH values. The successful formation of complexes is supported by mobility retardation in gel electrophoresis. A fluorescence assay[7,8] based on ethidium bromide displacement was used to study the kinetics of the strand invasion of duplex DNA by different bisPNAs, and this indicated that a two-step invasion process occurs. The results, interestingly, suggest that the preferred roles of arm A and arm B as WC or HG strands in bisPNA:DNA complexes is directed by the nature of the X substituent and the linker.

Results and Discussion

Synthesis of PNA Monomers, Linker and BisPNA Oligomers

The syntheses of protected *aep*PNA monomers 1-(*N*-Boc-aminoethyl)-4(*S*)-(N^4-benzyloxycarbonyl cytosin-1-yl)-2(*S*)-proline methyl ester (**1**), and 1-(*N*-Boc-aminoethyl)-4(*S*)-(N^2-isobutyrylguanin-7-yl)-2(*S*)-proline methyl ester (**2**) were performed according to our previously reported procedures (Figure 4).[8]

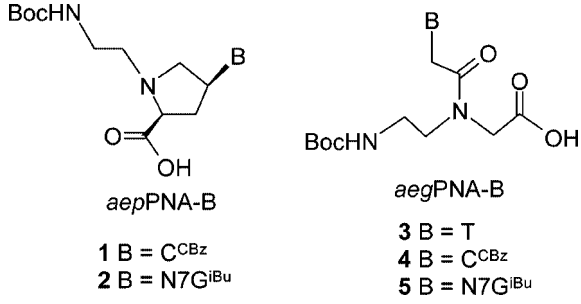

Figure 4. *aeg*-*aep*PNA monomeric units used in the synthesis of bisPNAs.

The *teg* linker **11** suitable for on-line coupling in PNA synthesis was obtained according to Scheme 1. Tetraethyl-

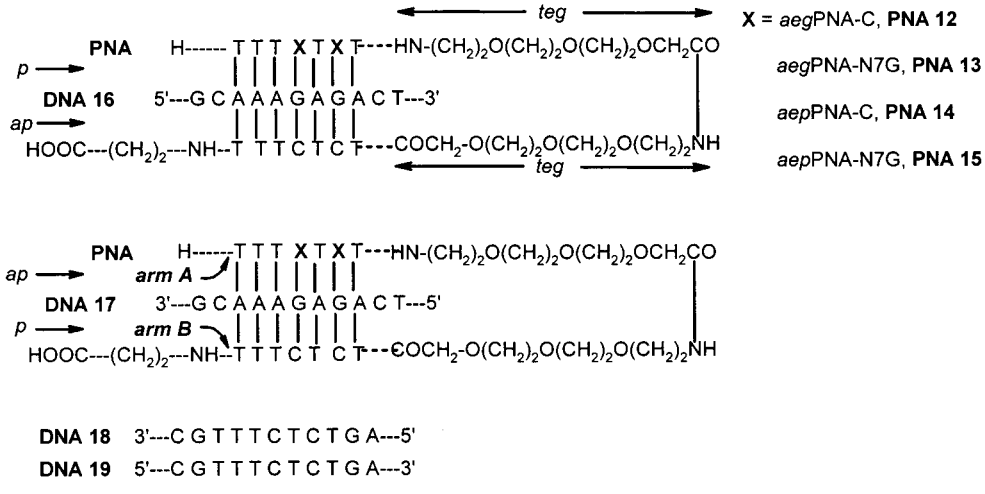

Figure 3. Design of hairpin bisPNAs.

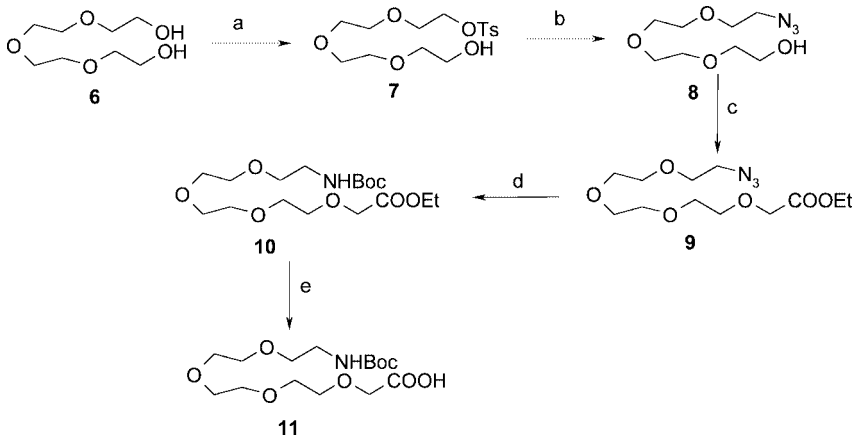

Scheme 1. a) *p*TsCl, NaOH, THF, Water, 0 °C, 3 h. b) NaN_3, DMF, 60 °C, 5 h. c) Br–CH_2–COOEt, NaH, DMF, 16 h. d) Ra/Ni, H_2, 40 psi, EtOAc, $(Boc)_2O$. e) aq. NaOH (1 M), MeOH.

ene glycol **6** was monotosylated[9] using *p*-toluenesulfonyl chloride followed by treatment with sodium azide in DMF to obtain the azide alcohol **8**. This was *O*-alkylated to the azido ester **9** with ethyl bromoacetate using sodium hydride, followed by hydrogenation to yield an intermediate amino ester, which was protected in situ with *t*-Boc using di-*tert*-butyl dicarbonate to obtain **10**. It was then hydrolyzed to the desired acid **11** and all compounds were characterized by appropriate spectroscopic data.

The hairpin bis PNA sequences (**12**–**15**) were designed to have *aeg*PNA-C (**12**), *aeg*PNA-N7G (**13**), *aep*PNA-C (**14**) and *aep*PNA-N7G (**15**) present in the arm A of the hairpin to bind DNA **16** in parallel and DNA **17** in antiparallel orientations. Consequently, the unmodified arm B of the hairpin would bind DNA **16** and DNA **17** in opposite antiparallel and parallel orientations, respectively. The different PNA and DNA oligomers that were synthesized are listed in Table 1.

Table 1. Hairpin bisPNA and DNA oligomers.[a]

PNA	Sequence composition
12	H–TTTCTCT–*teg*-*teg*–TCTCTTT–NH–$(CH_2)_2$–COOH
13	H–TTT ^{7}GT ^{7}GT–*teg*-*teg*–TCTCTTT–NH–$(CH_2)_2$–COOH
14	H–TTT c T c T–*teg*-*teg*–TCTCTTT–NH–$(CH_2)_2$–COOH
15	H–TTT ^{7}gT ^{7}gT–*teg*-*teg*–TCTCTTT–NH–$(CH_2)_2$–COOH
16	5′-G C A A A G A G A C T-3′
17	5′-T C A G A G A A A C G-3′
18	5′-A G T C T C T T T G C-3′ (complementary to **16**)
19	5′-C G T T T C T C T G A-3′ (complementary to **17**)

[a] T/C/^{7}G = *aeg*PNA-T/C/N7G; C/^{7}g = *aep*PNA-C/N7G, *teg*, linker.

The PNA oligomers were synthesized in a single assembly on Merrifield resin derivatized with β-alanine. Each coupling cycle involving successive deprotection, neutralization and coupling steps was monitored for efficiency by Kaiser's test. Tetraethylene glycol linker **11** was coupled using the same procedure employing HBTU, HOBt and diisopropylethylamine as the coupling agents. The oligomer synthesis was carried out starting from arm B of the hairpin, followed by the neutral linker and arm A in which *aeg*PNA-C, *aeg*PNA-N7G, *aep*PNA-C or *aep*PNA-N7G monomers are added in X positions and the synthesis was completed with other *aeg*PNA monomers. The oligomers were cleaved from the solid support using TFA-TFMSA[10] to yield PNAs with free "C" terminal carboxylic acids and simultaneous deprotection of the benzyloxycarbonyl groups on C. The N^2-isobutyryl groups of the N^7 of guanine were removed by further treatment with aqueous ammonia at 55 °C or with an ethylenediamine/ethanol mixture for 20 h.

The fully deprotected oligomers were desalted by size-exclusion chromatography over G25 Sephadex followed by purification using preparative reverse-phase HPLC on a C8 column. The purity of the oligomers was rechecked by analytical reverse-phase HPLC on a C18 column and their identity confirmed by MALDI-TOF mass spectrometry (see Supporting Information; for details see the footnote on the first page of this article).

UV-Melting

The oligodeoxynucleotides **16** and **17**, identical in sequence but reversed in a 5′-3′ direction, were used to probe the parallel/antiparallel binding preferences, studied by thermal UV melting experiments at pH 5.8 and 7.4. The hairpin bisPNA sequences **12**–**15** individually mixed with the oligonucleotides **16** or **17** in equimolar concentrations were annealed prior to melting. UV absorbances at 260 nm for the different bisPNA:DNA complexes were recorded as a function of temperature to generate percent hypochromicity-temperature plots (Figure 5). The UV melting temperature (T_m) values at pH 5.8 and 7.4 were deduced from maxima in the first derivative plots and are given in Table 2.

The control bisPNA **12** having the *aeg*PNA-C unit as X in arm A binds to either the parallel (*p*) DNA **16** or antiparallel (*ap*) DNA **17** (relative to arm A) at pH 7.4 with slightly different affinities (21 and 27 °C, respectively) (Entry 1, Table 2). At acidic pH 5.8, a higher T_m (29 and 42 °C) was seen with both DNA **16** and DNA **17** as expected from N3 protonation of cytosine and T_m with DNA **17** was significantly higher than that seen with DNA **16** [ΔT_m = 8 °C].

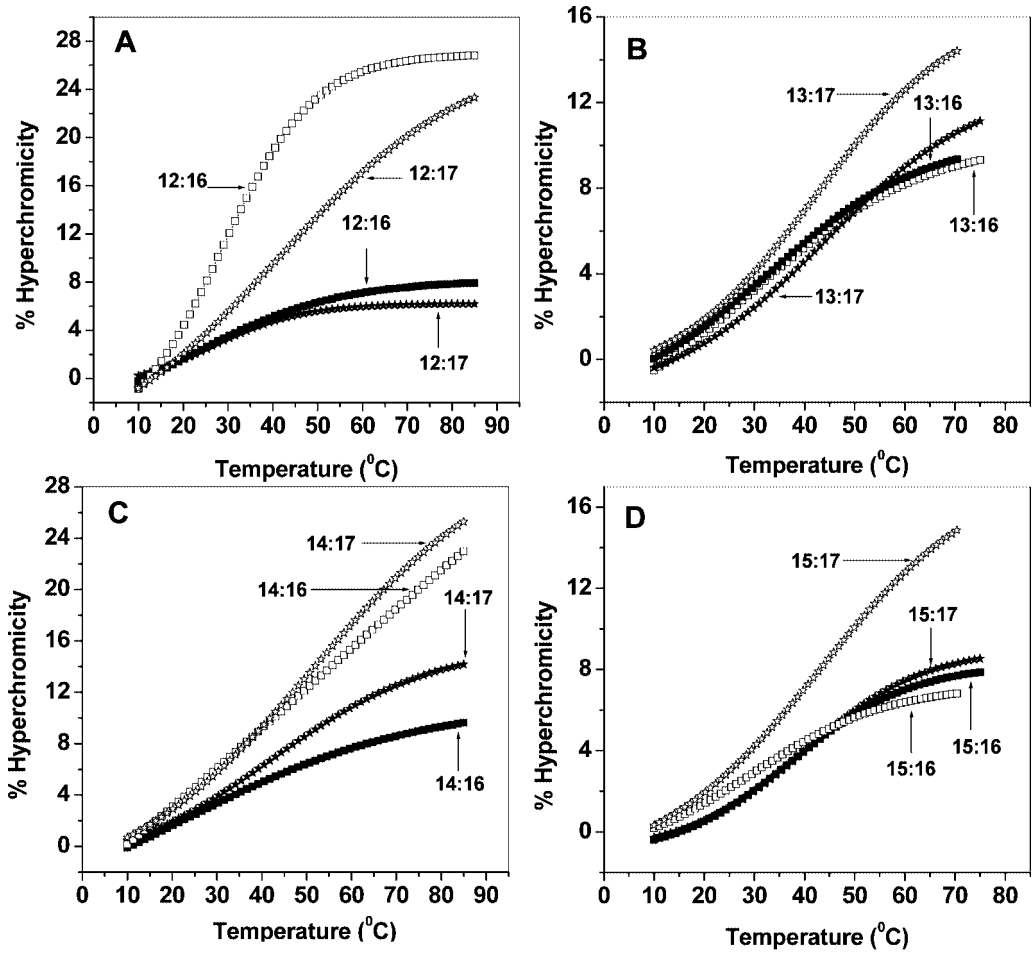

Figure 5. UV-T_m plots of the bisPNA:DNA complexes of (**A**) *aeg*PNA-C **12**, (**B**) *aeg*PNA-N7G **13** (**C**) *aep*PNA-C **14** (**D**) *aep*PNA-N7G **15** with DNA **16** and DNA **17**, at pH 5.8 (symbols: open squares, opens stars) and 7.4 (symbols: black filled squares, filled stars).

Table 2. UV-T_m of bisPNA-DNA complexes.[a]

Entry	PNA	DNA **16** (*p*)			DNA **17** (*ap*)		
		pH 7.4	pH 5.8	$\Delta T_{m(\Delta pH)}$	pH 7.4	pH 5.8	$\Delta T_{m(\Delta pH)}$
1	**12**, *aeg*PNA-C	21	29	+8	27	42	+15
2	**13**, *aeg*PNA-N7G	32	29	–3	44	41	–3
3	**14**, *aep*PNA-C	23	49	+26	42	52	+10
4	**15**, *aep*PNA-N7G	38	30	–8	41	44	+3

[a] UV-T_m data (°C) for PNA:DNA complexes with DNA **16** and **17**. Experiments were performed in 10 mM sodium phosphate buffer, pH 7.4 and 5.8. T_m values are accurate to ±1 °C and were obtained from peaks in the first derivative plots of percent hyperchromicity vs. temperature. Each experiment was repeated at least twice.

This protonation could be on the "C" located either in arm A or arm B of bisPNA **12**, with the protonated arm leading to HG and the nonprotonated arm to WC H bonding. The protonation of terminal, non-hydrogen bonded "C" in DNA **16** and **17** does not affect the binding or recognition event. Thus, in *aeg*PNA **12**, the two arms of bisPNA are distinguished in terms of binding in the WC or HG mode at pH 5.8, but it is not possible to assign the protonated HG strand.

The replacement of *aeg*PNA-C **12**, at X in arm A by the C^+ mimic *aeg*PNA-N7G (**13**) gave complexes of different stabilities (Entry 2, Table 2) with the target DNA strands **16** and **17**. At both pH values, a distinct preference was seen for binding of DNA **17** as compared to DNA **16** [ΔT_m = 12 °C] (Figure 4, B). The T_m was almost pH-independent with $\Delta T_m(\Delta pH)$ = –3 °C. The fact that N7G cannot bind in the WC mode, rules out arm B containing C to act as an HG strand. Thus, although donor-acceptor H-bonding sites of N7G recognize G in the HG binding mode in both *p* and *ap* orientations, the preferred binding mode is *ap*, with HG binding of arm A where N7G is located, leading to *p* WC binding of arm B.

At an acidic pH, a slight destabilization was seen suggesting that N3 protonation of cytosine is not favored in the arm B binding, in the *parallel* WC mode. In contrast to the achiral *aeg*PNA units, introduction of a chiral *aep*PNA-

C unit as X in arm A in bisPNA **14** leads to a significantly stronger binding at pH 7.4 with DNA **17**, as compared to binding with DNA **16** [Table 2, Entry 3, ΔT_m = 19 °C]. This suggests that chirality in *aep*PNA-C further influences the binding orientation preference. At pH 5.8, the thermal stability was significantly enhanced in the case of both DNA **16** and DNA **17**, resulting from the protonation of N3 of C [ΔT_m(ΔpH) = 26 and 10 °C, respectively]. The additional protonatable N on the pyrrolidine ring of *aep*PNA-C, with a higher pK_a (6.8) than that of N3 of C (4.5), may perhaps lead to the higher degree of stabilization seen at pH 5.8 (Figure 4, C). Since *aep*PNA-C on arm A cannot carry a positive charge simultaneously on both ring N and N3 of C, the preferred mode of binding is arm A in *ap* WC and protonated *aeg*-C in arm B in *p* HG.

The bisPNA **15** containing the non-protonatable chiral *aep*PNA-N7G unit as X in arm A exhibited a higher stability of derived complexes at neutral pH 7.4 relative to the chiral *aep*PNA-C **14**. The bisPNA **15** also formed more stable hybrids with DNA **17** than with DNA **16** at both pH values, with lower dependence of pH on T_m for DNA **17**, similar to *aeg*PNA-N7G **13** (Figure 5, D). This again suggested that arm A recognizes DNA **16** in *parallel* HG mode and **17** in *antiparallel* HG mode, with preferred binding in the latter orientation. The higher T_m of *aep*PNA-N7G perhaps arises from protonation of pyrrolidine ring N contributing to electrostatic stabilization. The overall results indicate that hairpin bisPNAs bind to DNA **17** better than they do to DNA **16**.

Fluorescence: Strand Invasion Assay

The bisPNA oligomers **12**–**15** are appropriate for studying the strand invasion properties by triplex formation when targeted towards duplex DNA. Ethidium bromide upon intercalation into a DNA duplex (**16**:**18** or **17**:**19**) shows an increase in fluorescence intensity[8] but is not known to interact with PNA_2:DNA or PNA:PNA complexes.[8,11] Strand invasion of the duplex DNA saturated with ethidium bromide by a triplex-forming PNA oligomer should therefore cause a decrease in ethidium bromide fluorescence due to the disruption of the DNA duplex-ethidium bromide complexation. The loss of ethidium bromide fluorescence as a function of time upon addition of triplex forming PNA oligomers may be used to study the kinetics of duplex strand invasion in this fluorescent intercalator displacement assay (Figure 6).

In our earlier studies with bisPNAs containing a cationic peptide linker[8] we noticed that the strand invasion is slower and incomplete in the case of *aeg*PNA-N7G and *aep*PNA at ambient temperature. These effects seem to arise due to conformational distortions induced in the PNA backbone by the *aep* chiral monomer units and also the presence of a purine base in a pyrimidine rich strand.

The DNA duplexes **16**:**18** and **17**:**19** were separately saturated with ethidium bromide and the kinetics of the strand invasion process was examined by monitoring the fluorescence emission decay at 590 nm (λ_{ex} = 490 nm) as a function of time after individually adding the four PNAs **12**–**15** for over 60 hours. The emission intensities in each case showed an exponential decrease at different rates eventually reaching a plateau (Figure 7 and Figure 8). Interestingly, the decay profiles of polyoxyethylene bisPNAs exhibited biphasic modes in contrast to the results from the cationic peptide linker[8] where the decay profile was clearly monophasic. In addition, the strand invasion also seems to go to completion. The present data on bisPNAs could be fitted into an exponential decay of second-order. Table 3 shows the two decay constants T_1 and T_2 computed from the data of Figure 7 and Figure 8.

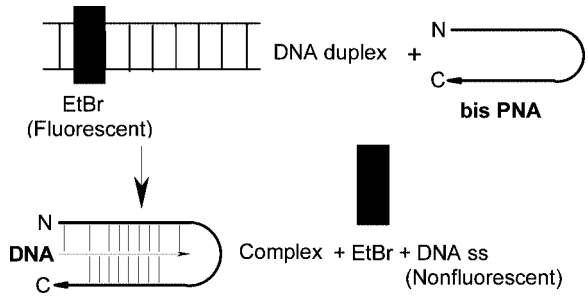

Figure 6. Principle of fluorescence assay for strand invasion.

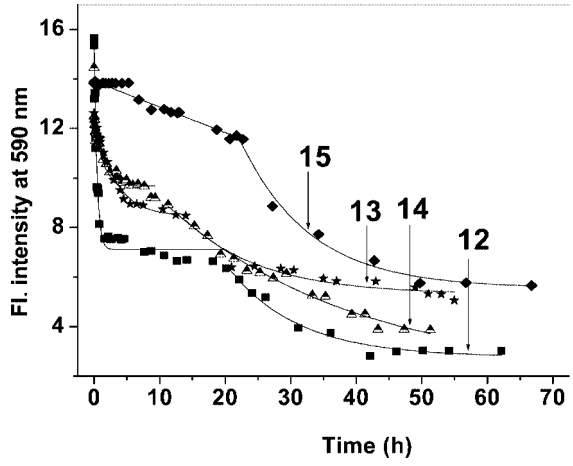

Figure 7. Ethidium bromide fluorescence as a function of time studied for the DNA duplex **16**:**18** after the addition of PNA **12**, PNA **13**, PNA **14** and PNA **15** at pH 7.4.

The data in Table 3 and Figure 7 and Figure 8 indicate that step 1 is a faster process compared to step 2 in all cases. For duplex invasion leading to triplexation with DNA **16** (Figure 7, Table 3), step 1 is fastest with *aeg*PNA-C **12** while slowest for *aeg*PNA-N7G **13**, with intermediate rates for *aep*PNAs **14** and **15**; step 2 is slowest in the case of *aep*PNA-C **14**, with other PNAs having similar rates.

In the case of duplex invasion generating triplexes with DNA **17** (Figure 8, Table 3), step 1 is fastest with *aep*PNA-N7G **15** while slowest for *aeg*PNA-N7G **13**, with intermediate rates for *aeg*PNA-C **12** and **14**. The decay kinetics follows an order completely different from that seen according to T_m. Thus the thermal stability of bisPNA:DNA duplexes seems to be disconnected from their kinetics of association/

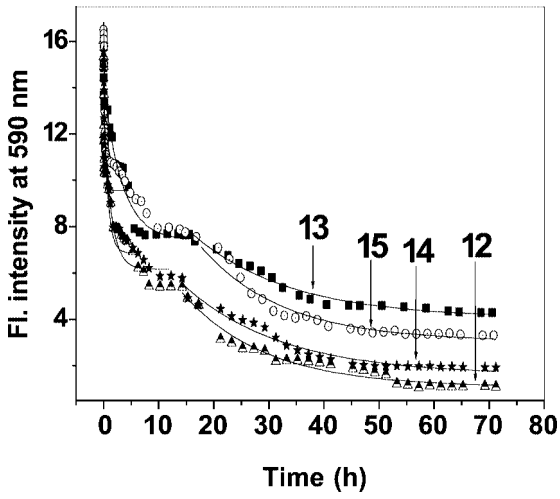

Figure 8. Ethidium bromide fluorescence as a function of time studied for the DNA duplex **17**:**19** after the addition of PNA **12**, PNA **13**, PNA **14** and PNA **15** at pH 7.4.

Table 3. Decay constants for duplex invasion by bisPNAs.[a]

DNA	**16:18**		**17:19**	
PNA	T_1	T_2	T_1	T_2
12	0.43	10.64	1.36	14.89
13	3.23	11.89	3.34	17.62
14	1.18	28.79	0.74	17.88
15	1.85	10.63	0.23	14.86

[a] Decay constants obtained from Figures 7 and 8 where results were subjected to non-linear curve fitting: exponential decay 2 in Microcal, origin 6.1 (T_1, T_2 given in hours).

dissociation. The faster rates of invasion seen in cationic linker bisPNA[8] may presumably be partly due to the electrostatic effects from the linker, which repels the positively charged ethidium bromide. The triplex formation with bisPNA was found to be a one-step process. The DNA duplex invasion by polyoxyethylene-linked bisPNA occurs in two steps that can be kinetically delineated in contrast to a single-step process observed for cationic peptide linked bisPNA.

Gel Shift Assays: Competition Binding Experiments

Electrophoretic gel shift assay was used to establish the formation of bisPNA:DNA complexes. The electrophoretic mobility of a DNA fragment in a native polyacrylamide gel is retarded upon complexation with PNA and hence can be used to study the strand.

The PNAs were individually treated with dsDNA and the complexation was monitored by nondenaturing gel electrophoresis at 10 °C. The spots were visualized on a fluorescent TLC background. The formation of PNA:DNA triplexes is accompanied by displacement of one strand of dsDNA and the appearance of a lower migrating band due to PNA:DNA complexes.

Figure 9 shows the results of competition binding experiments carried out by adding hairpin bisPNAs to the DNA duplex (**16**:**18** or **17**:**19**) followed by annealing and complexation monitored by nondenaturing gel electrophoresis at 10 °C. Due to a higher binding affinity of PNA:DNA complexes compared with DNA:DNA complexes, the added PNA binds to the complementary DNA **16**:**17** in the DNA triplex, releasing the DNA strand **18**:**19**. This is clearly seen in the gel electrophoresis in which the DNA duplex band is converted into a bisPNA:DNA complex seen as a retarded band and the released DNA strand is seen as a faster moving band (Figure 9, Lane 1–2, 4–5 and Lane 7–9). The results unambiguously prove that PNAs do competitively displace one strand of a DNA duplex to form a complex with the other complementary strand. The mobility difference seen for ds- and ssDNA is highlighted in the supplementary information.

Discussion

Entropic enhancement of strand invasion efficiency is possible by use of PNA clamps or bisPNAs in which two homopyrimidine PNA oligomers are covalently connected by a flexible loop.[12,13] Such linking of two PNA oligomers reduces a trimolecular reaction of 2 × PNA and 1 × DNA to a PNA-DNA bimolecular reaction, accelerating the PNA invasion.[14] PNA strand invasion of dsDNA has been shown to be accelerated by incorporation of positive charges into PNA or bisPNA oligomers.[15] The use of bisPNAs wherein the Watson–Crick PNA strand is connected through ethylene glycol linkers to the Hoogsteen PNA strand[10,13] offers interesting possibilities of incorporating neutral mimitics into either of the PNA segments to examine the relative orientations of the WC and HG pairing strands. It has been found that the selectivity in PNA:DNA complex formation is orientation-directed with the Watson–Crick strand in the antiparallel configuration relative to DNA and the Hoogsteen strand in the parallel configuration.

N7-Glycosylated guanine is a positional isomer of the naturally occurring N9-guanine and recognises the target G:C base pair occurring in major grooves through bidentate hydrogen bonding. Being neutral, it surpasses the requirement of acidic pH for triplexation.[16–18] N7G can mimic protonated cytosine in the pyrimidine motif forming stable triplexes at neutral pH with the recognition of C only being through the HG mode in either parallel and antiparallel orientations[13] (Figure 10). However, G is not recognised in the WC binding mode. Thus incorporation of N7G units in PNA stabilizes the triplex only when engaged in the HG mode unlike C or J bases.

UV-T_m studies suggest that T_m for the interaction of bisPNA-C (**12** and **14**) with DNA depends significantly on pH, while this is relatively insignificant for PNA-N7G (**13** and **15**). The pH-dependent T_m clearly arises from the necessity for N3C protonation, which should occur in arm A of bisPNA-C complexes of DNA **16** and arm B for bisPNA complexes of DNA **17**. In bisPNAs of N7G, the arm A always binds in the HG mode, since no pH-dependent T_m was observed.

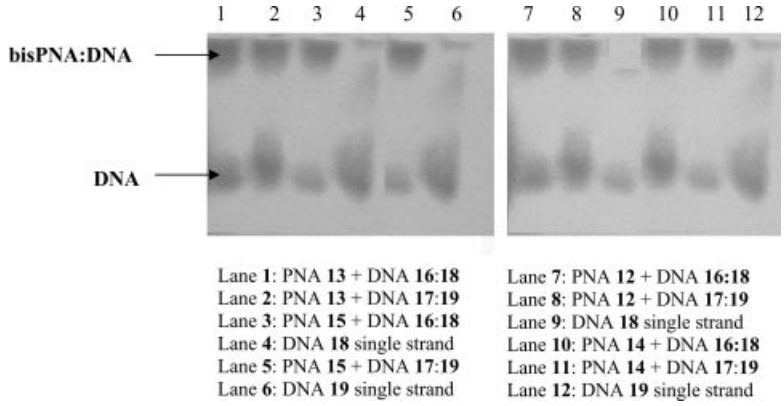

Figure 9. 15% Polyacrylamide gel electrophoresis of PNA:DNA complexes.

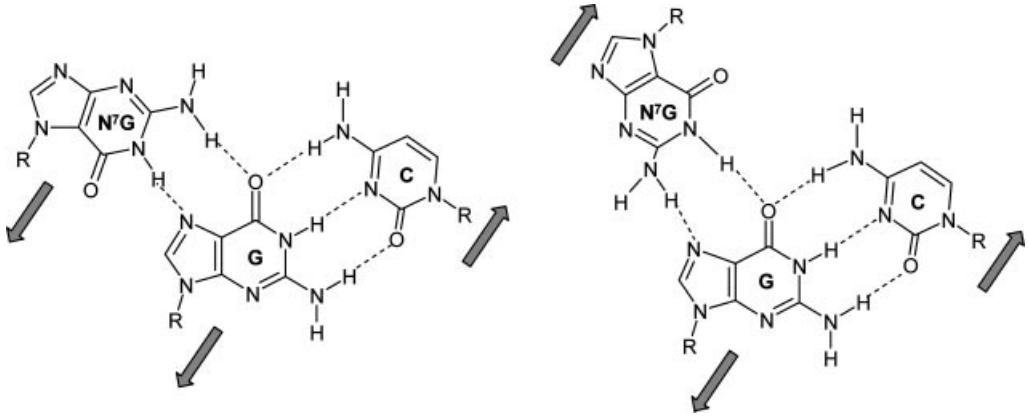

Figure 10. N7G third strand binding in the parallel and antiparallel HG mode.

The pK_a's of cytosine N3 in *aeg*PNA-C (3.6) and *aep*PNA-C (3.47) were not very different, though slightly lower than N3–C in cytidine (4.34). The pK_a of the pyrrolidine ring is 6.7 and thus in the *aep*PNA-C, the protonation of N3 of C is electrostatically unfavored due to the prior protonation of the pyrrolidine ring nitrogen (pK_a = 6.7). Thus, it is likely that C in arm B is protonated leading to HG binding. The overall results suggest that N7G in the X position favors arm A binding in the HG mode while *aep*-PNA C in the X position favors arm A in the WC mode of binding.

In the literature, two plausible routes for the strand invasion reaction have been postulated[19–21] According to one mechanism (Figure 11), the first stage consists of a fluctuating opening of the DNA double helix and a transient formation of a PNA:DNA Watson–Crick duplex (WC first mechanism).

The second mechanism envisages the formation of an unstable PNA:DNA_2 triplex through Hoogsteen pairing (HG first mechanism), followed by dissociation of the duplex to form a PNA_2:DNA triplex. The final outcome is the same for both mechanisms and the unstable intermediates are difficult to detect. By using pH-dependent gel mobility shift analysis, it was demonstrated[21] that at neutral pH, C-containing PNAs undergo strand invasion by the HG first mechanism (Figure 11).

Our present results based on the fluorescence assay give direct and strong support for a two-step process, as seen by the observance of biexponential decay. The initial step is a kinetically faster process over 0.2–3.4 h, while the second

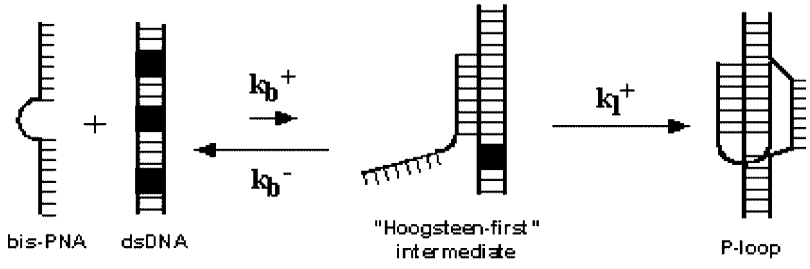

Figure 11. Proposed Hoogsteen-first mechanism in strand invasion of homopyrimidine bisPNAs into dsDNA.[21]

step is slower over a subsequent 10.6 to 28.7 h. Compared to *aeg*PNA **12**, the *aep*PNAs **14** and **15** show a T_1 that is three times lower, perhaps due to the presence of the rigid pyrrolidine ring as part of the backbone, which sterically slows down the initial binding of the PNA to DNA duplex. The PNA **13** having *aeg*PNA-N7G was the slowest, perhaps due to additional energy barriers in the interconversion of *syn-anti* rotamers in attaining hybridization competent conformations. The *aep*-PNAs **14** and **15** having the base directly linked to the pyrrolidine rings lack such rotamers. The first step in the case of *aep*-bisPNA-N7G was quite fast and the second step of base pair formation was inordinately slow for *aep*-bisPNA-C **14**, for which, the reasons are not obvious from present experiments.

In the first step both DNA duplexes **16**:**18** and **17**:**19** should form transient HG pairing with arm A of bisPNAs **12**–**15**, while the second step involves formation of WC pairing. For the duplex invasion of **17**:**19** by bisPNAs, which also leads to more stable hybrids, it was noticed that the *aep*PNAs exhibit faster kinetics for the first step. The first HG mechanism gives rise to antiparallel binding with the DNA duplex, which is more favorable than the relatively slower HG parallel binding seen for the **16**:**18** DNA duplex. For *aeg*-bisPNA, the first HG binding was faster in the parallel mode than the antiparallel. Thus our results seem to delineate the invasion process by parallel/antiparallel binding, with the latter being more favorable.

Conclusions

The N7G nucleobase and neutral *teg* linker has been successfully incorporated into PNA using simple chemistry and solid-phase peptide synthesis. It has proved to be a good C^+ mimetic at neutral and acidic pH, with differences in T_m being observed for DNA **16** and DNA **17**. The overall results suggest that bisPNAs bind better to DNA **17** than DNA **16**. Thus, triplex formation is pH dependent when *aeg*/*aep*PNA-C units are used, while *aeg*/*aep*PNA-N7G units permit triplex formation at physiological pH as well as at acidic pH.

In addition, the introduction of *aep*PNA C units into the backbone of the hairpin bisPNAs that form triplexes, strongly influences the recognition of DNA in an orientation-selective manner. The more stable complexes were formed when the arm A was antiparallel to the central strand. In summary (i) the *aeg*PNA HG strand prefers to be *ap* to the DNA strand (ii) the effect is more pronounced when X is the chiral *aep*PNA unit (iii) *aep*PNA C has much a higher UV-T_m at acidic pH values due to protonation of the pyrrolidine ring nitrogen in the WC mode of binding and (iv) the triplex formation by bisPNAs is a two-step process which is discernible when the cationic linker is replaced by a neutral *teg*-*teg* linker. The topological issues of specificity in PNA_2:DNA triplex formation in bisPNA are thus resolved by employing the chiral protonatable unit *aep*PNA-C and the protonated C mimic *aep*PNA-N7G.

Experimental Section

N^2-Isobutyrylguanine,[8] 1-(*N*-Boc-aminoethyl)-4-(*R*)-hydroxy-2-(*S*)-proline methyl ester,[17] 1-(*N*-Boc-aminoethyl)-4-(*R*)-O-mesyl-2-(*S*)-proline methyl ester,[8] 1-(*N*-Boc-aminoethyl)-4-(*S*)-(N^4-benzyloxycarbonyl-cytosin-1-yl)-2-(*S*)-proline methyl ester,[8] 1-(*N*-Boc-aminoethyl)-4-(*S*)-(N^2-isobutyrylguanin-7-yl)-2-(*S*)-proline methyl ester,[8] were prepared according to literature procedures. The synthesis of the *aeg*PNA-T/C monomers was carried out according to the procedures described earlier.

2-{2-[2-(2-Hydroxyethoxy)ethoxy]ethoxy}ethyl 4-Methylbenzenesulfonate(7):[9] A solution of sodium hydroxide (2.74 g, 68.5 mmol) in water (15 mL) was added to a mixture of tetraethylene glycol (**6**) (87.8 g, 452 mmol) and THF (15 mL). After the mixture had cooled down to 0 °C, a solution of *p*-toluenesulfonyl chloride (8.3 g, 43.7 mmol) in THF (50 mL) was added while stirring for 1 h. After stirring at 0 °C for 2 h, the reaction mixture was poured into ice water (250 mL). The organic layer was separated, and the aqueous layer was extracted with CH_2Cl_2 (3 × 100 mL). The combined organic layers were washed twice with water (50 mL). Drying of the organic layer and evaporation of the solvent under reduced pressure afforded (13.74 g, 90% yield with reference to tosyl chloride) of clear oil **7**. ^{1}H NMR ($CDCl_3$): δ = 7.86–7.76 (d, 2 H), 7.35–7.31 (d, 2 H), 4.17–4.12 (m, 2 H), 3.70–3.58 (m, 14 H), 2.43 (s, 3 H) ppm.

2-{2-[2-(2-Azidoethoxy)ethoxy]ethoxy}ethanol (8): Monotosylate **7** (5 g, 14.4 mmol) in dry DMF (50 mL) was added to sodium azide (4.67 g, 71.85 mmol). The reaction mixture was heated at 60 °C while stirring for 5 h. The solvent was removed under vacuum; the residue was placed in water and extracted with CH_2Cl_2 (3 × 50 mL). The pooled organic extracts were washed with water and brine. Drying of the organic layer and evaporation of the solvent under reduced pressure afforded azide **8** (2.70 g, 87% yield). ^{1}H NMR ($CDCl_3$): δ = 3.69–3.46 (m, 14 H), 3.39–3.36 (t, 2 H) ppm. ^{13}C NMR ($CDCl_3$): δ = 71.41, 69.43, 68.77, 60.28, 59.76, 49.47 ppm. IR ($CHCl_3$): 2106 cm^{-1} and others.

Ethyl 14-Azido-3,6,9,12-tetraoxatetradecan-1-oate (9): A solution of azide **8** (3.50 g, 16 mmol) in dry DMF (5 mL) was added to a cooled solution of sodium hydride (0.42 g, 17.58 mmol) in dry DMF (10 mL). The reaction mixture was stirred for 30 min and then ethyl bromoacetate (1.96 mL, 17.5 mmol) was added dropwise, at 0 °C. The reaction mixture was stirred for 16 h at room temperature. The reaction mixture was quenched with ice water and solvent was removed under vacuum; the residue was placed in water and extracted with ethyl acetate (3 × 50 mL). The pooled organic extracts were washed with water and brine. Drying of the organic layer and evaporation of the solvent gave crude oil. Purification using column chromatography afforded **9** (2.0 g, 44% yield). ^{1}H NMR ($CDCl_3$): δ = 4.26–4.12 (m, 4 H), 3.69–3.46 (m, 14 H), 3.39–3.36 (m, 2 H), 1.29–1.21 (t, 3 H) ppm.

Ethyl 14-*tert*-Butoxycarbonylamino-3,6,9,12-tetraoxatetradecan-1-oate (10): Compound **9** (2 g, 6.6 mmol) was placed in dry ethyl acetate (2 mL) in a 250 mL hydrogenation flask and di-*tert*-butyl dicarbonate (1.57 g, 7.2 mmol) was added to it. Raney Ni (1 mL, suspension in ethanol) was separately washed thoroughly with ethyl acetate and was added to the hydrogenation flask. It was subjected to hydrogenation at 40-psi pressure for 1.5 h. The catalyst was filtered and washed with methanol/ethyl acetate mixture. The filtrate was concentrated under vacuum to give the crude protected amine. Purification using column chromatography afforded **10** (1.5 g, 50% yield). ^{1}H NMR ($CDCl_3$): δ = 5.20 (br. s, 1 H), 4.24–4.09 (m, 4 H), 3.69–3.46 (m, 14 H), 3.27–3.24 (m, 2 H), 1.38 (s, 9 H), 1.26–1.19

(t, 3 H) ppm. ^{13}C NMR ($CDCl_3$): δ = 170.11, 155.74, 78.69, 70.53, 70.20, 69.87, 68.33, 60.42, 40.10, 28.08, 13.85 ppm. MS: (ESI) 379 $(M)^+$, 279 (M^+ – Boc).

14-*tert*-Butoxycarbonylamino-3,6,9,12-tetraoxatetradecan-1-oic Acid (11): Aqueous 2 M NaOH (2 mL) was added to a solution of Ethyl 14-*tert*-butoxycarbonylamino-3,6,9,12-tetraoxatetradecan-1-oate **10** (0.4 g, 1.0 mmol) in methanol (2 mL). TLC analysis after 10 min indicated the absence of the starting material as a result of hydrolysis of the methyl ester function. The excess NaOH was neutralized by Dowex-50 H^+ resin, which was then filtered off. The methanol from the filtrate was removed under vacuum and concentrated it to dryness to obtain the product **11** (0.35 g, quantitative yield) as a brown solid. ^{1}H NMR ($CDCl_3$): δ = 6.00 (br. s, 1 H), 4.11 (s, 2 H), 3.69–3.46 (m, 14 H), 3.34–3.24 (m, 2 H), 1.39 (s, 9 H) ppm. ^{13}C NMR ($CDCl_3$): δ = 170.11, 155.74, 79.29, 71.18, 70.56, 70.27, 69.11, 40.35, 28.39 ppm. MS: (ESI) 352 $(M)^+H$, 252 (M^+H – Boc).

UV-Melting: The concentration of the PNA oligomers was calculated on the basis of the absorption at 260 nm, assuming the molar extinction coefficients of the nucleobases to be as in DNA, i.e., T, 8.8 $L{\cdot}cm^{-1}{\cdot}mol^{-1}$; C, 7.3 $L{\cdot}cm^{-1}{\cdot}mol^{-1}$; G, 11.7 $L{\cdot}cm^{-1}{\cdot}mol^{-1}$ and A, 15.4 $L{\cdot}cm^{-1}{\cdot}mol^{-1}$. The hairpin PNA oligomers (**12**–**15**) and the relevant complementary DNA oligonucleotide (**16/17**) were mixed together in a 1:1 molar ratio in 0.01 M sodium phosphate buffer, pH 5.8 or 7.4 to obtain a final strand concentration of 1 μM. The samples were annealed by heating at 85 °C for 1–2 min, followed by slow cooling to room temperature. They were kept at room temperature for 30 min and then, refrigerated overnight. UV experiments were performed with a Perkin–Elmer λ35 UV/Vis spectrophotometer fitted with a Peltier temperature programmer. The samples were heated at a rate of 0.2 °C per minute and the absorbance was recorded at every minute at 260 nm. The percent hyperchromicity at 260 nm was plotted as a function of temperature and the melting temperature was deduced from the peak in the first derivative plots.

Fluorescence Assay for Strand Invasion: Fluorescence measurements were performed with a Perkin–Elmer model LS-50B spectrometer attached to a Julabo water bath circulator for variable temperature. The DNA duplex **16**:**18/17**:**19** (1 μM) in a 5 mM sodium phosphate buffer, pH 7.4 at 20 °C was saturated with ethidium bromide (0.5 μM) and then excited at 490 nm and the emission monitored at 590 nm using a spectral bandwidth of 5 nm. The kinetics of the strand invasion process was then examined by monitoring the fluorescence decay at 590 nm as a function of time after individually adding the four bisPNAs **12**–**15** (10 μM) for over 60 h.

Supporting Information Available (see also footnote on the first page of this article): (1) HPLC profiles of PNA oligomers **12**–**15**. (2) Mass spectra of PNAs **12**–**15** (3) NMR spectra of compounds **7**–**11**. (4) Mass spectra of compounds **2**, **5**, **10**–**11**. (5) Gel electrophoresis of DNA complexes.

Acknowledgments

P.S.S. thanks CSIR, New Delhi for the award of a senior research fellowship. V.A.K. acknowledges DST, New Delhi, for a research grant. K.N.G. is an Honorary Professor at Jawaharlal Nehru Centre for Advanced Scientific Research, Bangalore.

[1] M. Egholm, O. Buchardt, L. Christensen, C. Behrens, S. M. Freier, D. A. Driver, R. H. Berg, S. K. Kim, B. Norden, P. E. Nielsen, *Nature* **1993**, *365*, 566–568.
[2] D. R. Corey, *Trends Biotechnol.* **1997**, *15*, 224–229.
[3] L. Good, P. E. Nielsen, *Antisense Nucleic Acid Drug Dev.* **1997**, *7*, 431–437.
[4] *ap*: PNA N-terminus towards the 3′-end and C-terminus towards the 5′-end of cDNA/RNA); *p*, PNA N-terminus towards the 5′-end and C-terminus towards the 3′-end of cDNA/RNA).
[5] M. Egholm, O. Buchardt, P. E. Nielsen, R. H. Beg, *J. Am. Chem. Soc.* **1992**, *114*, 9677–9678.
[6] P. S. Miller, P. Bhan, C. D. Cushman, T. L. Trapane, *Biochemistry* **1992**, *31*, 6788–6793.
[7] C. R. Woods, T. Ishii, B. Wu, K. W. Bair, D. L. Boger, *J. Am. Chem. Soc.* **2002**, *124*, 2148–2152.
[8] M. D′Costa, V. A. Kumar, K. N. Ganesh, *J. Org. Chem.* **2003**, *68*, 4439–4445.
[9] M. Smet, W. Dehaen, *Molecules* **2000**, *5*, 620–628.
[10] R. S. Hodges, R. B. Merrifield, *Anal. Biochem.* **1975**, *65*, 241–272.
[11] W. C. Tse, D. L. Boger, *Acc. Chem. Res.* **2004**, *37*, 61–69.
[12] M. Egholm, L. Christensen, K. L. Dueholm, O. Buchardt, J. Coull, P. E. Nielsen, *Nucleic Acids Res.* **1995**, *23*, 217–222.
[13] M. C. Griffith, L. M. Risen, M. J. Greig, E. A. Lesnik, K. G. Sprankle, R. H. Griffey, J. S. Kiely, S. M. Freier, *J. Am. Chem. Soc.* **1995**, *117*, 831–832.
[14] H. Kuhn, V. V. Demidov, M. D. Frank-Kamenetskii, P. E. Nielsen, *Nucleic Acids Res.* **1998**, *26*, 582–587.
[15] A. G. Veselkov, V. V. Demidov, P. E. Nielsen, M. D. Frank-Kamenetskii, *Nucleic Acids Res.* **1996**, *24*, 2483–2488.
[16] T. S. Rao, R. H. Durland, G. R. Revankar, *J. Heterocycl. Chem.* **1994**, *31*, 935–940.
[17] J. Hunziker, E. S. Priestley, H. Brunar, P. B. Dervan, *J. Am. Chem. Soc.* **1995**, *117*, 2661–2662.
[18] H. Brunar, P. B. Dervan, *Nucleic Acids Res.* **1996**, *24*, 1987–1991.
[19] S. T. Crooke, B. Lebleu, *Antisense Research and Applications*, CRC Press, Boca Raton, FL, **1993**.
[20] V. V. Demidov, M. V. Yavnilovich, B. P. Belotserkovskii, M. D. Frank-Kamenetskii, P. E. Nielsen, *Proc. Natl. Acad. Sci. USA* **1995**, *92*, 2637–2641.
[21] H. Kuhn, V. V. Demidov, P. E. Nielsen, M. D. Frank-Kamenetskii, *J. Mol. Biol.* **1999**, *286*, 1337–1345.

Received: July 20, 2005
Published Online: October 13, 2005

